ISSN 2522-3488 Vol. 7, Issue 6: 51-59, DOI: 10.25236/IJNDES.2023.070609

Research on the Changes in the Ecological Landscape Pattern and the Benefits Functions of Flood Control in the Dasi River Basin

Gaoyang Sui[1,a,*], Li Yu[2,b]

[1]*Shandong Survey and Design Institute of Water Conservancy Co, LTD, Jinan, Shandong, China*
[2]*Jinan Hydrological Centre, Jinan, Shandong, China*
[a]*423636050@qq.com*, [b]*423636050@qq.com*
[*]*Corresponding author*

Abstract: *Water ecological health and safety assessment is the core of water ecological security research, and it is a powerful tool for discovering and addressing safety hazards in the water environment. Water ecological environment protection is a systemic issue that crosses scales and regions. It not only involves the protection of the water ecosystem itself but also extends to the interaction between the entire urban area and the water environment. Therefore, achieving water ecological health and safety requires not only attention to water quantity and quality related to water resources supply and demand and water pollution caused by urbanization but also the comprehensive consideration of the stability of the ecosystem structure caused by land use activities and its ability to provide the necessary well-being benefits for human production and life stability. This plays a crucial role in maintaining regional water environment and economic and social stability in the long term.*

Keywords: *Water Conservancy Project Construction, Water Resources, Flood Prevention*

1. Research Overview

Studying the water ecological health and safety status of the Dasi River Basin (initial section) can help decision-makers gain a better understanding of the regional water ecological system's health status, changes in trends and influencing factors over the past few decades, identify water ecological environmental issues in the area, and propose necessary corresponding policies and water ecological resilience restoration strategies to effectively prevent risks. [1] The research findings are of significant theoretical significance and practical value in promoting the high-quality development of the Shandong Peninsula urban agglomeration, and establishing a new demonstration for ecological protection and high-quality development in the Yellow River Basin.

1.1. Research Content

Analyze the changes in ecosystem landscape patterns, flood effects, and the impacts on human well-being and benefits caused by land use changes [2].

1.2. Primary Economic, Social, and Environmental Benefits

This study utilizes GIS (Geographic Information System) and remote sensing techniques to analyze the impacts of land use activities resulting from the economic and social development in the study area on landscape structure, flood hydrological processes, and ecosystem services. [3] Furthermore, it establishes a pressure-structure-process-function framework to assess the water ecological health and safety from multiple dimensions. [4] The study completes the assessment of regional water ecological health conditions and proposes a water ecological resilience restoration model, which is beneficial for promoting the coordinated development of the environment and economy in the area.

ISSN 2522-3488 Vol. 7, Issue 6: 51-59, DOI: 10.25236/IJNDES.2023.070609

2. Research Findings

2.1. Water Environmental Characteristics of the Study Area.

2.1.1. Regional Overview

The geographical location of the Dasi River Basin (initial section) is between 36°45′32″N~36°54′54″N and 116°59′8″E~117°5′6″E, with an area of 75.49 km2 (is shown in Figure 1). Over the years, with the development of urbanization, there have been significant changes in land use types. [5] The region belongs to the typical alluvial plain area of the Yellow River and has been repeatedly impacted by floods caused by the breach of the Yellow River in history.

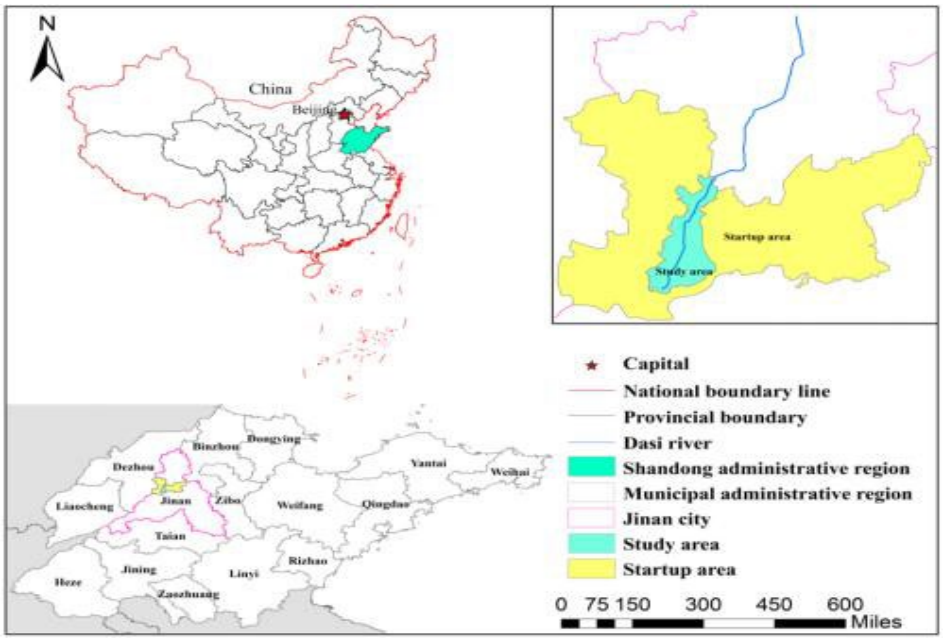

Figure 1: Geographical location map of the Dasi River Basin (initial section)

2.2. Climate Characteristics

The climate characteristics are hot summers and cold winters, with concentrated rainfall. It belongs to the northern warm temperate semi-humid monsoon climate. The wind direction changes with the seasons. In winter and summer, the prevailing wind direction is north-south, while in spring and autumn, the wind direction varies. [6] The annual average temperature is about 13.6℃, the annual average precipitation is about 685 mm, and the annual total sunshine duration is about 2347.10 hours.

2.3. Analysis of Land Use Change

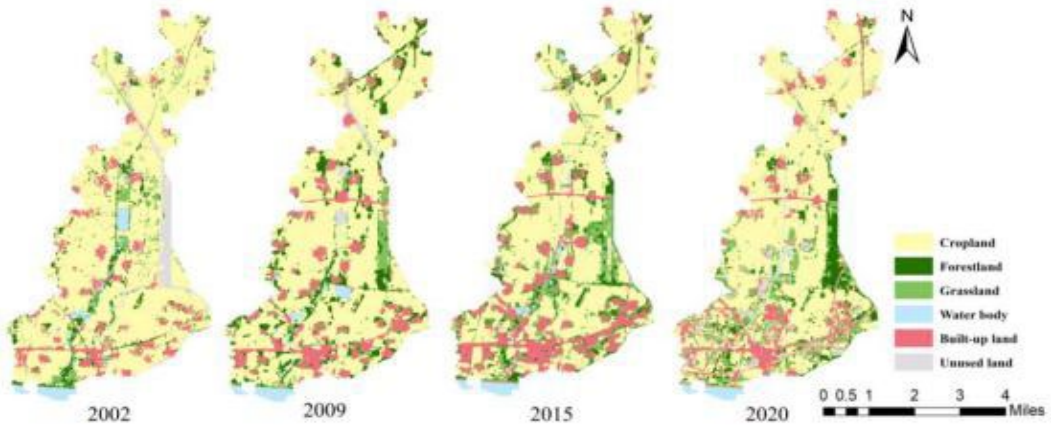

Figure 2: Spatial distribution maps of land use in the study area from 2002 to 2020

ISSN 2522-3488 Vol. 7, Issue 6: 51-59, DOI: 10.25236/IJNDES.2023.070609

First, radiometric calibration and atmospheric correction are carried out on the remote sensing image data used to improve the accuracy and quality of the images. [7] Next, the study area is clipped using the vector polygon of the Dasigou River Basin (initial section) as a mask. [8] Then, using ENVI software, ROIs (Region of Interest) for various land use types are established to extract the land use information for the years 2002, 2009, 2015, and 2020 using supervised classification methods. [9] Finally, a comparative analysis is conducted on the results of the supervised classification to obtain the temporal sequence of land use changes in the study area, as shown in Figure 2 and Table 1.

Table 1: Land use area and proportion by land use type

Year	Cropland	Forestland	Grassland	Water body	Built-up land	Bare land
2002	Area (ha) 5471.57	456.41	354.42	276.35	661.07	329.02
2009		4888.46	760.26	597.13	210.53	974.52
2015		4329.63	548.16	1099.26	245.74	1288.03
2020		4703.94	642.07	811.48	239.65	952.31
2002-2009	Area changes (ha)	-583.11	303.85	242.71	-65.82	313.45
2009-2015		-558.83	-212.10	502.13	35.21	313.51
2015-2020		374.31	93.91	-287.78	-6.09	-335.72
2002-2020		-767.63	185.66	457.06	-36.70	291.24
2002-2009	Change rate (%)	-1.52	9.51	9.78	-3.40	6.77
2009-2015		-1.91	-4.65	14.02	2.79	5.36
2015-2020		1.73	3.43	-5.24	-0.50	-5.21
2002-2020		-0.78	2.26	7.16	-0.74	2.45

In 2002, 2009, 2015, and 2020, arable land was the main substrate in the study area, accounting for 72.48%, 64.76%, 57.35%, and 62.31% of the total area, respectively. During the study period, the area of arable land and bare land showed a decreasing trend followed by an increasing trend, while the area of grassland and built-up land showed an increasing trend followed by a decreasing trend. The water bodies showed a minor decrease. From the perspective of annual change rate, although the area of grassland is not significant, it is the land use type with the most significant change during the study period, with an annual change rate of 7.16%, followed by built-up land with an annual change rate of 2.45%. The annual change rates of forest land and bare land are similar but in opposite directions, at 2.26% and -2.19% respectively. The annual change rates of arable land and water bodies are the lowest, at -0.78% and -0.74% respectively.

In order to scientifically understand the process of landscape pattern changes caused by human-induced land use activities in the Dasi River Basin (starting section) from 2002 to 2015, landscape pattern characteristics analysis was conducted using four landscape characteristics: landscape area/edge, shape, aggregation, and diversity. The fragstats 4.3 software was used to select landscape indices for landscape pattern analysis at the landscape level.

Table 2: Presents landscape pattern indices at the landscape level in the study area for the years 2002-2020

Year	AREA_MN (hm^2)	LPI (%)	PD (each/hm^2)	ED (m/hm^2)	SHAPE_MN	COHESION	CONTAG (%)	SHDI
2002	11.3252	29.6718	4.1358	25.0506	1.1679	97.9562	51.9195	1.0218
2009	10.2252	22.3261	4.5699	26.8066	1.1776	96.1568	47.0406	1.1381
2015	7.6315	21.9810	6.1386	33.1511	1.1961	95.6808	41.0172	1.2347

According to Table 2, from the analysis of area/density/edge characteristics, the average patch area (AREA_MN) and the largest patch index (LPI) both show a decreasing trend from 2002 to 2015, while patch density (PD) shows an increasing trend. This indicates that over the 13-year period, there was a noticeable phenomenon of large and intact patches being fragmented in the study area. The dominant landscape areas decreased, the number of patches per unit area increased, and the degree of fragmentation increased.

3. Flood Simulation Analysis in the Study Area

3.1. The Necessity of Flood Simulation Research

The dashe River is a tributary of the Tuai River, with no embankments along its entire course. It is a

ISSN 2522-3488 Vol. 7, Issue 6: 51-59, DOI: 10.25236/IJNDES.2023.070609

natural spillway formed by multiple breaches of the Yellow River in history, allowing floodwater to flow into the Tuai River and erode its channel. As the main drainage channel within Jiyang District, it is responsible for drainage in six towns including Cuizhai, Huihe, Suomiao, and Jiyang, as well as the discharge of tailwater from five towns in the Yellow River irrigation area. In this study area, rainfall during the flood season is concentrated and often includes heavy rainstorms. The regional slope is relatively gentle, resulting in slow runoff speed and a long duration of the flood peak. In the event of continuous heavy rain, the previous peak has not subsided before the subsequent one arrives, often forming compound peaks or consecutive peaks, posing significant threats to the safety of people's lives and property in the region [10].

At the same time, the study area is located in the central area of the starting area and is also a key region for future planning and development. The development of urbanization will inevitably lead to an increase in the degree of land hardening in the region, increasing the potential harm caused by flood disasters resulting from rainfall runoff. Conducting flood simulation research, identifying high-risk flood areas, and analyzing the relationship between these areas and changes in land use are of practical significance for flood disaster warning, stormwater management, and achieving high-quality development in the Yellow River Basin [11].

3.2. Source of Data

The DEM (Digital Elevation Model) data in the study area are obtained from the Geographic Spatial Data Cloud. The rainfall data are obtained from the temporal rainfall data of hydrological stations near the study area (36.683°N, 116.983°E).

3.3. Research Methods

The DEM (Digital Elevation Model) data in the study area from 2002 to 2020 are sourced from the Geographic Spatial Data Cloud. During the acquisition process, they are subject to geometric deformations caused by factors such as sensor system errors, sensor platform instability, and variations in scale due to surface terrain fluctuations. In order to eliminate the image errors caused by these geometric deformations, orthorectification must be performed. Orthorectification is the process of stretching the image, taking into account the position, elevation, and sensor information, to ensure its spatial accuracy with the map.

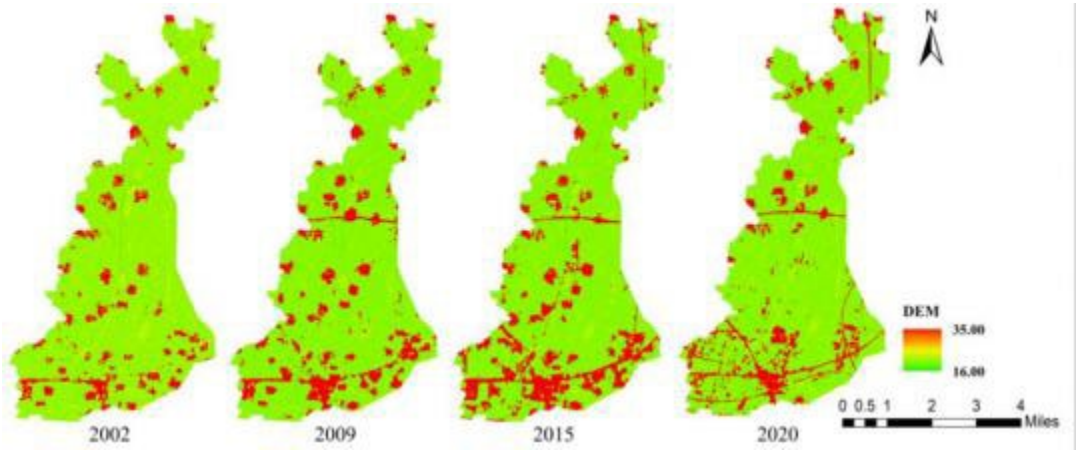

Figure 3: Corrected DEM

By comparing the elevations of multiple construction sites in the DEM, it was found that the elevation difference between the construction sites and the surrounding areas was less than 2.00m, which does not match the actual situation. Therefore, to highlight the water resistance ability of the buildings, the elevation of the construction land in the DEM was uniformly raised to 35.00m. For highlighting the flood-carrying capacity of the roads, considering that the curbs of the roads are generally 0.15m high, the road elevations were adjusted by lowering them by 0.15m.

By comparing the elevations of the riverbed of the Dasi River in multiple locations on the topographic map with actual measured elevation data, it was found that the average elevation of the riverbed on the topographic map was 1.50m higher than the actual measured elevation of the Dasi River. Therefore, the elevation of the Dasi River was adjusted by lowering it by 1.5m. After these

ISSN 2522-3488 Vol. 7, Issue 6: 51-59, DOI: 10.25236/IJNDES.2023.070609

adjustments, the DEM data were corrected is shown in Figure 3.

In order to analyze the impact of land use changes from 2002 to 2020 on flood risk in the study area, considering the planning data of the study area, the rainfall return period P for four years is set to 50 years, and the rainfall duration is set to 1 hour. The rainfall intensity formula used is the Jinan City rainfall intensity formula (Chicago method). The Jinan City rainfall intensity formula is as follows:

$$q=1421.481(1+0.932\log r) \quad (1)$$

$$(t+7.347)0.617 \quad (2)$$

In the formula: q represents the rainfall intensity in mm/min; P represents the return period, with a value of 50 years; t represents the rainfall duration, with a value of 1 hour. The rainfall design scenario.

3.4. Results and Analysis

In the study of flood problems, a common issue often encountered is the lack of sufficient observational data for simulation. This problem is also present in this study. However, a rationality analysis based on the simulated scenario results indicates that the constructed model for runoff coefficient and runoff processes are within reasonable ranges. Overall, the simulation results are in good agreement with statistical data and can be used for further research on flood issues in the study area.

The simulated distribution of flood disasters, peak flood discharge, and peak flood area in different time periods in the study area are analyzed. In order to highlight the distribution of different flood levels on the image map, areas with water depths below 0.10m in the level 5 flood category are considered as risk-free areas and not displayed. By combining the four-period spatial distribution maps of floods, the modified DEM data, and the land use map, it can be observed that the flood-prone areas in the study area have shifted to some extent with changes in land structure over time.

In 2002, the western and eastern regions of the study area had relatively higher flood risk levels. This was mainly due to the higher impervious surface area and smaller runoff coefficient in those areas, resulting in increased surface runoff. From 2002 to 2009, the peak flood discharge and peak flood area in the study area showed a decreasing trend. This was primarily attributed to the implementation of ecological protection projects such as returning cultivated land to forests or grasslands, which increased the overall permeability of the region through the expansion of forest and grassland areas, leading to a reduction in the comprehensive runoff coefficient. Additionally, the surrounding forest and grassland landscapes with poor permeability around construction land improved, enhancing the infiltration capacity and controlling the amount of floodwater.

From 2009 to 2015, rapid economic and social development inevitably encroached on some ecological land. The construction of residential areas, roads, bridges, and other infrastructure led to an increase in impervious surfaces. At the same time, mismanagement of some forest land resources led to regression in certain areas, resulting in obvious floods on both sides of the river channels. During this period, the peak flood discharge and peak flood area increased by 12.42% and 11.57%, respectively.

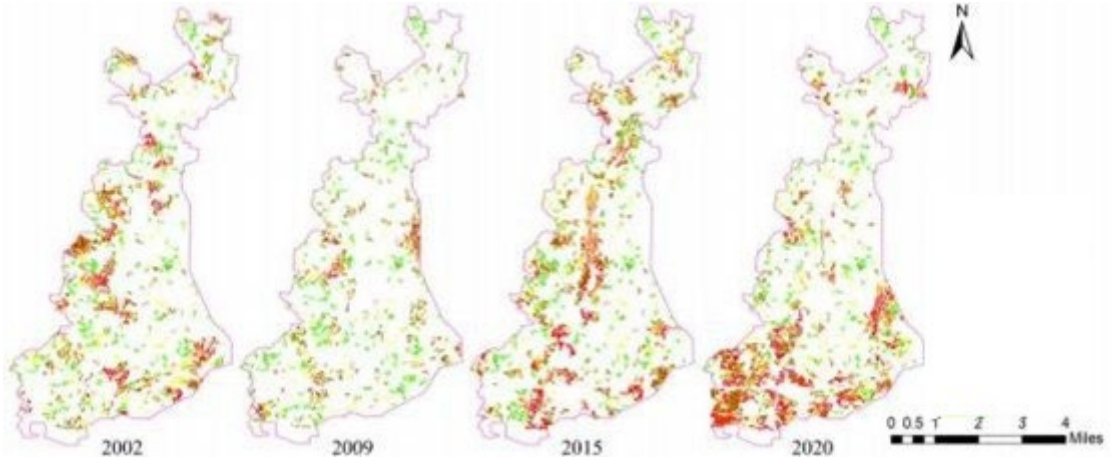

Figure 4: Spatial Distribution of Floods in the Study Area from 2002 to 2020

From 2015 to 2020, the southern part of the study area showed an increasing trend in flood risk.

ISSN 2522-3488 Vol. 7, Issue 6: 51-59, DOI: 10.25236/IJNDES.2023.070609

This was mainly due to the demolition of old residential areas, road reconstruction, and upgrades, which led to a reduction in forest and grassland areas and an increased fragmentation level, resulting in a weakened flood-carrying capacity. Conversely, the central and northern parts of the study area experienced a reduction in flood risk. This was primarily attributed to land consolidation and ecological civilization construction projects, which resulted in a more regular and even distribution of farmland, an increase in the dominance of forest and grassland, a reduction in fragmentation, and an enhancement in flood-carrying capacity. Overall, the peak flood discharge and peak flood area showed a decreasing trend during this period is shown in figure 4.

4. Sensitivity and Transfer Study of Different Rainfall Durations and Return Periods on Flood Risk in the Southern (Bridge Section) of the Study Area

From the spatial distribution map of floods during the period from 2002 to 2020, it can be observed that the high-risk areas of floods have a tendency to shift towards the southern part of the study area. Considering the land spatial planning documents of the starting area (2021-2035), it is known that the southern part of the study area will be a key focus for future development and construction of the bridge section. It is of great significance to conduct in-depth research on the influences of different rainfall durations and return periods on the occurrence of flood risks in this area for disaster prevention and mitigation, as well as to ensure the stable and sustainable development of human society in this region.

4.1. Data Source

The Digital Elevation Model (DEM) and the data of the Dasi River cross-section were provided by the Construction Management Department of the Jinan New and Old Kinetic Energy Conversion Starting Area. The DEM has a resolution of 10m. Land use types, river data, and other vector data were extracted from a raster satellite image with a pixel resolution of 0.12m in 2021. Rainfall data was obtained from the time-rainfall data of hydrological stations near the research area (36.683°N, 116.983°E). The water depth data of the extreme heavy rain on July 18, 2007, was obtained through field surveys, as well as from relevant online media and news reports.

4.2. Research Methodology

To explore the impact of different rainfall durations and return periods on regional flood risk, this study adopts the Jinan City Rainstorm Intensity Formula (commonly known as the Chicago Method) to design rainfall patterns. The Jinan City Rainstorm Intensity Formula is as follows:

$$q = 1421.481(1+ 0.932 \log r) \tag{3}$$

$$(t + 7.347)0.617 \tag{4}$$

In the formula: q represents rainfall intensity in mm/min; P represents return period in years; t represents rainfall duration in minutes. The calculated return periods are 1 year, 3 years, 5 years, 10 years, 20 years, 50 years, and 100 years. When the rainfall duration is 1 hour, the corresponding rainfall amounts are 38.40mm, 55.48mm, 63.42mm, 74.20mm, 84.98mm, 99.22mm, and 110.00mm. When the rainfall duration is 2 hours, the rainfall amounts are 51.55mm, 74.48mm, 85.14mm, 99.61mm, 114.07mm, 133.20mm, and 147.66mm. When the rainfall duration is 3 hours, the rainfall amounts are 60.86mm, 87.92mm, 100.50mm, 117.58mm, 134.66mm, 157.22mm, and 174.30mm. The rainfall peak coefficient is set at 0.347.

4.3. Results and Analysis

In studying flood problems, a lack of sufficient observational data is a widespread issue in simulations, which is also present in this study. To validate the reasonableness of the model parameters, the simulated results of urban waterlogging during the "718" heavy rainfall event in Jinan City in 2007 were selected for evaluation.

(1) Spatial Distribution of Flood Levels

According to the document "Spatial Planning for the Conversion of New and Old Kinetic Energy in the Starting Area of Jinan" (2021-2035), it is known that the southern part of the study area is a key area for future urban construction in the Daqiao District of Jinan. Therefore, the focus of this study is to

ISSN 2522-3488 Vol. 7, Issue 6: 51-59, DOI: 10.25236/IJNDES.2023.070609

conduct a detailed analysis of the distribution of flood disasters in the area where the southern part of the study area intersects with the Daqiao District, under different rainfall scenarios. Under the same rainfall duration, the risk area continues to increase as the return period of rainfall increases. Under the same return period, the risk area increases as the rainfall duration increases. Combined with the current land use status map of the Daqiao District, it is known that the 1st level risk area mainly appears on urban roads and spreads outwards with the increase of return period and rainfall duration. The 5th level risk area is mainly distributed in areas with low runoff coefficients such as farmland, green areas, and forests, and also spreads outwards with the increase of return period and rainfall duration. Furthermore, according to the elevation spatial distribution map obtained by interpolating elevation points in the Daqiao District, it can be observed that within the study area, each risk level shows an increasing trend centered around low-lying areas and spreads outwards with the increase of return period and rainfall duration, gradually "absorbing" the surrounding areas.

Under the same rainfall duration conditions, the peak total water volume increases with the increase of the return period. Taking a rainfall duration of 3 hours as an example, under the same rainfall duration, the maximum difference in the peak total water volume ratio (calculated by dividing the difference between the two values by the maximum value to represent the degree of difference) for return periods of 1 year, 3 years, 5 years, 10 years, 20 years, 50 years, and 100 years are 76.32%, 64.09%, 57.12%, 45.42%, 30.65%, 12.16%, and 0.00% respectively.

At the same time, the peak total water volume corresponding to each risk level also gradually increases with the return period, but the rate of increase decreases with the increase of the return period. Moreover, the higher the risk level, the larger the rate of increase.

Under the same rainfall duration conditions, the peak total water volume for each risk level increases with the increase of rainfall, but the rate of increase decreases with the increase of rainfall duration. The variations of the water depths for risk levels 2, 3, 4, and 5, and the average water depth, are not significant with changes in rainfall duration and return period. The corresponding average water depths are 0.46m, 0.32m, 0.20m, 0.12m, and 0.19m, respectively. The water depth for risk level 1 fluctuates more significantly under different return periods, but overall it increases with the increase of the return period. The peak area of regional water accumulation under the same rainfall duration and return period is as shown in Table 3.

Table 3: Peak Water Accumulation Area for Each Flood Level under Design Rainfall Scenarios Unit: hectares

Time	Period	Flood grade and magnitude									
		1	incre	2	incre	3	incre	4	incre	5	incre
1h	1a	0.88		1.10		5.96		41.50		63.15	
	3a	1.28	45.45%	2.64	140.00%	15.07	152.85%	81.89	97.33%	104.73	65.84%
	5a	1.38	7.81%	3.11	17.80%	18.53	22.96%	97.06	18.52%	130.11	24.23%
	10a	1.58	14.46%	3.97	27.65%	24.89	34.32%	124.30	28.06%	174.67	34.25%
	20a	1.58	0.15%	4.46	12.34%	27.67	11.17%	156.38	25.81%	210.28	20.39%
	50a	2.01	26.84%	6.81	52.69%	43.77	58.17%	204.33	30.66%	241.46	14.83%
	100a	2.36	17.58%	8.81	29.37%	57.18	30.65%	247.88	21.32%	251.09	3.99%
	1a 3a	1.54		3.58		19.93		85.44		106.27	
	5a	1.60	3.96%	4.17	16.48%	26.10	30.96%	125.03	46.33%	165.65	55.87%
		1.99	24.53%	6.26	50.12%	36.54	40.00%	158.48	26.75%	192.03	15.92%
2h	10a	2.19	9.69%	9.35	49.31%	48.65	33.14%	203.42	28.36%	232.52	21.09%
	20a	2.62	19.91%	13.26	41.82%	62.97	29.44%	261.95	28.77%	243.17	4.58%
	50a	2.77	5.74%	19.54	47.38%	80.70	28.15%	346.38	32.23%	229.01	-5.82%
	100a	3.57	28.67%	25.53	30.70%	100.86	24.98%	369.64	6.72%	224.44	-2.00%
	1a	2.10		4.70		26.15		96.74		101.77	
3h	3a	2.18	4.19%	6.16	31.06%	35.19	34.56%	145.14	50.04%	173.36	70.34%
	5a	2.41	10.20%	10.28	66.95%	44.31	25.93%	167.28	15.25%	198.83	14.70%
	10a	2.86	18.97%	14.75	43.38%	54.20	22.32%	228.18	36.40%	227.56	14.45%
	20a	3.43	19.61%	24.54	66.44%	64.27	18.58%	298.53	30.83%	246.47	8.31%
	50a	6.61	93.05%	35.84	46.02%	106.03	64.99%	360.30	20.69%	240.35	-2.48%
	100a	8.70	31.65%	43.27	20.74%	142.53	34.42%	385.71	7.05%	236.46	-1.62%

Analysis from Table 3 shows that under the same rainfall duration, the peak area of accumulated water for each flood grade gradually increases with the increasing grade. At the same time, the peak area of accumulated water for flood risk levels 1, 2, 3, and 4 continuously increases with the increasing

ISSN 2522-3488 Vol. 7, Issue 6: 51-59, DOI: 10.25236/IJNDES.2023.070609

rainfall return period, while the peak area of accumulated water for risk level 5 shows a decreasing trend with the increasing return period. This is mainly caused by low-water-level overflow. However, the increase rate of the peak area of accumulated water for each risk level decreases with the increasing return period. Under the same return period, the peak area of accumulated water for each flood grade increases with the increasing rainfall duration, showing an overall increasing trend. When the rainfall duration is 3 hours, the average increase rates of the peak area of accumulated water for risk levels 1, 2, 3, 4, and 5 are 29.61%, 45.76%, 33.46%, 26.71%, and 17.28% respectively. This indicates that the peak area of accumulated water for risk level 2 is the most sensitive to the changes in the return period, while the peak area of accumulated water for risk level 5 is the least sensitive. Taking the increase rate changes of each risk level from the 50-year return period to the 100-year return period as an example, the difference in the increase rates of the peak area of accumulated water for risk levels 1, 2, 3, 4, and 5 between the 1-hour rainfall duration and the 2-hour rainfall duration, as well as between the 2-hour rainfall duration and the 3-hour rainfall duration, are 8.10%, 11.30%, -15.10%, -14.94%, and -6.36%, respectively. This indicates that the peak area of accumulated water for risk levels 1 and 2 is more sensitive to short-duration rainfall, while the peak area of accumulated water for risk levels 3, 4, and 5 is more sensitive to long-duration rainfall.

5. Conclusion

During the research period, there have been significant changes in land use in the study area. Balancing economic benefits and ecological benefits is of great significance for achieving sustainable development in the starting area. In the future development of the starting area, the government should further strengthen the protection of ecological land and limit the uncontrolled expansion of construction land. In addition, it is important to recognize the importance of farmland as the main land use type in the study area in balancing economic development and environmental protection. By establishing brand agricultural demonstration zones, agriculture can be combined with ecotourism. At the same time, in order to encourage agricultural production and safeguard food security, the government should further implement various agricultural preferential policies and encourage the development of green ecological and circular agriculture, such as high-quality and high-yield specialty agriculture, which can effectively promote the sustainable development of rural economy and natural environment. In terms of forest resources, the government should strengthen the protection and restoration of natural forests and promote the transformation to high-productivity and high-energy forests. At the same time, efforts should continue to be made in returning farmland to forests and grassland, and to guide the orderly movement of the population. In areas with strong human activity disturbance and low ecological service levels, such as densely built areas and wastelands, the government can establish ecological corridors to enhance information exchange and energy transfer among species in the community, and promote harmonious development between humans and nature. In addition, special projects such as flood control, drainage, river channel regulation, and the restoration of saline-alkali land should be carried out to maintain ecological security. Based on the spatial distribution of ESVS, ecological protection red lines can be delineated to effectively identify key areas for environmental protection. This is of great significance for guiding the rational land spatial planning in the starting area and ensuring high-quality development in the Yellow River Basin.

References

[1] Kao, J. Application of Grouting Anti-Seepage Treatment Technology in Risk Removal and Reinforcement Construction of Reservoirs. China High-Tech and High-Tech Enterprises, (2021), 115(07), 108-109.

[2] Liu, J. Research on Construction Techniques and Anti-Seepage Reinforcement Treatment of Reservoirs. Development Guidance of Building Materials, (2012), 20(24), 120-122.

[3] Bhre Wangsa Lenggana. Construction of Road Drainage System Based on Remote Sensing Technology and Support Vector Machine Algorithm. Water Pollution Prevention and Control Project, (2022), Vol. 3, Issue 1: 32-41. https://doi.org/10.38007/WPPCP.2022.030104.

[4] Huang, Y. Reliability Analysis of Concrete Anti-Seepage Wall in Reservoir Reinforcement Engineering Based on High-Pressure Rotary Jet Grouting Technology. Groundwater, (2021), 43(02), 192-195.

[5] Mo, H., & Chen, Y. Application of Grouting Anti-Seepage in Risk Removal and Reinforcement Engineering of Xinchongkeng Reservoir. Science, Technology, Innovation, and Application, (2022), 12(24), 193-196.

ISSN 2522-3488 Vol. 7, Issue 6: 51-59, DOI: 10.25236/IJNDES.2023.070609

[6] Huang, Z. Application of High-Pressure Jet Grouting Technology in Anti-Seepage Reinforcement Construction of Reservoir Dams. Building Materials and Decoration, (2016), No. 412(08), 275-276.
[7] Zhang, T. Application Study of High-Pressure Rotary Jet Anti-Seepage Wall Construction Technology in Yuanyangchi Reservoir. Gansu Water Resources and Hydropower Technology, (2022), 58(11), 60-64.
[8] Asiane Ullah. Dynamic Distributed Based on PLC Software Redundancy. Distributed Processing System, (2022), Vol. 3, Issue 4: 61-69. https://doi.org/10.38007/DPS.2022.030408.
[9] He, C., Liu, M., Zhang, Y., Wang, Z., Hsiang, S. M., Chen, G., and Chen, J., 2022. Exploit Social Distancing in Construction Scheduling: Visualize and Optimize Space–Time–Workforce Tradeoff. Journal of Management in Engineering, 38(4), 4022027. DOI: https://doi. org/ 10. 1061/ (ASCE)ME. 1943-5479. 0001037.
[10] Athanasios V. Serafeim. Four Ecological Strategies for Urban Natural Environment Protection. Nature Environmental Protection (2020), Vol. 1, Issue 1: 1-9. https://doi. org /10. 38007/ NEP. 2020. 010101.
[11] Ernest Foomen. Nanotechnology in Environmental Biotechnology. Academic Journal of Environmental Biology (2020), Vol. 1, Issue 4: 1-8. https://doi. org/10. 38007/AJEB. 2020. 010401.